J.Chem.Soc.Pak., Vol. 38, No. 04, 2016

# Adsorption of Alizarin and Fluorescein Dyes onto Palm Seeds Activated Carbon: Kinetic and Thermodynamic Studies

[1]Nasiru Abdus-Salam and [2]Magaji Buhari
*[1]Department of Chemistry, University of Ilorin, P.M.B. 1515, Ilorin, Nigeria.*
*Department of Chemistry, Gombe State University, P.M.B. 127, Gombe, Nigeria.*
nasalami2002@yahoo.co.uk*

(Received on 16th July 2013, accepted in revised form 16th May 2016)

**Summary:** Activated carbon was prepared from date palm seed using one step procedure with 56.54 % efficiency, 2.89 % ash content, 781.40 $m^2 g^{-1}$ surface area, 711.2 mg $g^{-1}$ iodine number and the CHN analysis gave 69.25 % C, 3.91% H and 1.56% N. The FTIR spectroscopy revealed O-H, C-H, C≡C, C=C and C-O stretching; XRF revealed P, Ca, Si, S and K as major elements. The influences of agitation time, initial dye concentration, adsorbent dose and temperature were studied in batch experiments. A 57.78% Alizarin and 68.40% Fluorescein removal were attained within the first 15 min of agitation. Kinetic studies showed good correlation coefficient for pseudo-first and pseudo-second order kinetic models. The adsorption data fitted well into Langmuir isotherm than Freundlich isotherms with correlation coefficient ($R^2$) very close to unity and Langmuir maximum adsorption constant, $q_m$ > 1000. The Freundlich coefficients relating to overall adsorption capacity, $K_f$ (mg $g^{-1}$) is 197.65 and 396.28 and surface heterogeneity, n is 3.34 and 3.18 for Alizarin and Fluorescein respectively. The activation energy ($E_a$) of the adsorption process of alizarin and fluorescein on DPA were found to be -8.19 and +21.43 Kj $mol^{-1}$ respectively. The evaluation of the thermodynamic quantities showed that the adsorption process was spontaneous and endothermic.

Keywords: Alizarin dye; Fluorescein dye; Adsorption, Kinetics; Thermodynamics; Activated carbon.

## Introduction

In Nigeria like any other developing nations, the demand for activated carbon (AC), is met through importation at a very high cost and depletion of foreign reserve, whereas vast quantities of agricultural by-products which can be used for its production are generated annually. If sourced locally and technology is developed, it will create wealth from waste and reduce over dependent on importation by converting these materials considered by-products into activated carbon adsorbents, which can be used for water and wastewater treatment [1] to remove hazardous organic compounds or those that impart odour or taste [2]. An effluent from textile industry is often highly loaded with mixtures of dyes, acids, bases, inorganics, and toxic organics and dissolved solids [3, 4] which make the removal by biological process difficult. The chemical structures of some commercially available textile dyes are: (a) Alizarin (anthraquinone dye) and (b) Fluorescein (triarylmethane dye).

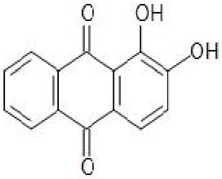

Fig 1: (a): Chemical structure of Alizarin.

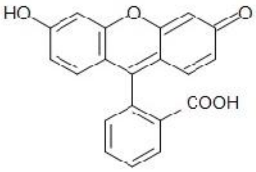

Fig 1: (b): Chemical structure of Fluorescein.

Alizarin is insoluble in water but soluble in aqueous alkaline solutions in the pH range 7.82 - 12.87. At pH below 5.2 most alizarin can be present in the form of yellow-coloured undissociated molecules. At pH between 6.8 and 10.1 most alizarin can occur as red monovalent anions. Above pH 12.1, alizarin dissociates into divalent anions with a blue-violet colour [5]. In the case of fluorescein, the $pK_a$ of the OH group attached to the xanthene moiety can be 6.43. At pH 9.1, fluorescein exists purely as dianion specie [6]. Effluents from textile industries contain these dyes and the colour impacted onto water is highly visible even at relatively low concentrations. Consequently, such discharge into natural bodies of water diminishes the aesthetic, biological and chemical qualities of water bodies. It could also pose health risk to aquatic lives because of their persistence and non-biodegradable characteristics [7]. Consequently, the removal of colour from effluents containing various kinds of

---

*To whom all correspondence should be addressed.

synthetic dyes becomes imperative. The methods of colour removal from industrial effluents include biological treatment, coagulation, floatation, adsorption, oxidation and hyper filtration [7]. Among the treatment options, adsorption appears to have considerable potential for the removal of colour from industrial effluents. Adsorption onto activated carbons is a well-known process for micro-pollutants removal [8]. AC is suitable as an adsorbent because it seldomly fouled by chemicals, has lower sensitivity to daily climatic change (diurnal variation), an excellent adsorbent for organic pollutants and possess great packing flexibility in design operation [9].

A carbon activation (AC) using chemical activating agents is a new generation of adsorption fibre development. Sorbents obtained with this method provides higher yield, high surface area, high mesopores volumes and some unusual pore surface chemistries [10, 11]. Adsorption is greatly influenced by the nature and the amount of the surface functional groups such as phenolic, carboxylate, lactones, quinines which are introduced by the activating agent during activation process [12].

AC also contain physical characteristic such as extensive internal pore structure that develops during the activation process and internal surface area. Some of the literatures on AC include those prepared from Barhi date seeds for removing 2,4-dichlorophenoxyacetic acid (2,4-D) herbicide was determined from batch tests [13]. Thermodynamic parameters such as standard enthalpy ($\Delta H^o$), standard entropy ($\Delta S^o$) and standard free energy ($\Delta G^o$) were evaluated. Raw date palm seeds were used as precursor for preparation of an effective adsorbent for the removal of sulphate from aqueous solution [14], adsorption of phenol from wastewater on date seed carbon (DSC) [15], Alizarin, Eriochrome Blue Black R and Fluorescein adsorption on chitosan, goethite and magnetite as adsorbents were investigated [4], adsorption of alizarin yellow from aqueous solution by wood charcoal [16].

Some other agricultural by-products that have been used for the preparation of AC include rubber wood sawdust [17], dates stone [18], bamboo-based 19], coconut shell [20, 21]. There are wide variations in the adsorptive properties of AC prepared from different agricultural base which is essentially due to the optimization of preparation conditions [22]. Activated carbon with a relatively wide pore size distribution can be obtained solely through a chemical activation process [22]. Physical activation can further enhance the adsorbent‘s pore structure due to a partial oxidation of the carbonized material by gases such as $CO/CO_2$ or steam [23].

The aim of the study was to explore the feasibility of preparing activated carbon from a waste agricultural by-product, the Date palm seed (DPS) for the removal of Alizarin and Fluorescein dyes from solutions and also to optimize the adsorption conditions that will ensure high dyes uptake. The kinetics and thermodynamics of the adsorption processes were studied in order to establish the efficiency and the feasibility of using DPA as an adsorbent.

## Experimental

### *Sample Collection and Pre-treatment*

The date palm seeds were collected from popular ‘Ipata’ market in Ilorin, the samples were washed with distilled water to remove all impurities, sun dried and cracked using hammer. The resulting cracked seeds were sun-dried again for 3 days for proper drying. All reagents that were used in this study were of analytical grade. Working standard solutions were prepared from analytical grade reagents and by serial dilution from the stock solution.

### *Production of Activated Carbon*

A single-step production was adopted where by carbonization and activation by thermal decomposition of the raw material already impregnated with activating agent was carried out. A 65 g of the raw DPS was soaked 100 ml of 50 % (v/v) $H_3PO_4$ acid at room temperature for 48 hr, the phosphoric acid was decanted and the impregnated sample was washed thoroughly with deionised water until the pH reading was slightly basic (7.8). The impregnated raw material was carbonized in a muffle furnace at 400 °C for 90 minutes. After cooling, the carbonized material was weighed to determine percentage yield then pulverised to reduce the size and sieved using a 100 µm sized sieve. Thereafter, samples with diameter ≤ 100 µm were used for other determinations and experiments.

### *Characterization*

The DPA efficiency was determined by mass difference between the starting raw DPS and the DPA obtained [53]. The DPA moisture content were determined by oven drying at 103 $^{O}$C [54], the volatile organic matter by American society for Testing and Materials [54], the ash content was determined at 625 $^{O}C$ [55], surface area by titration [45], Bulk density by using density bottle [56], thermometric determination of pH in $CO_2$ free water [57] and the iodine number by ASTM procedure [58]. The carbon, hydrogen and nitrogen were analysed by CHN CE 440 analyser, metals composition by XRF axios pw: 4400/24 model and the surface functional groups by Perkin Elmer model 100.

*Determination of Adsorption Capacity*

A 50 ml of varying concentrations of the dyes (2, 5, 10, 15, 20, 30 and 50 mg $L^{-1}$) were contacted with 1g of the adsorbent. The contents were agitated on an incubator shaker, KBLEE1001 for a period of 8 hr. The un-adsorbed dye was determined with Beckman Coulter, DU-730 life science UV/Vis spectrophometer. The quantity sorbed was calculated from eqn. 7 [59].

$$q_e = \frac{C_i - C_f}{M} \times V \qquad (07)$$

where $q_e$ is the quantity of dye adsorbed (mg $L^{-1}$), $C_i$ and $C_f$ are the initial and final concentration of the dyes (mg $L^{-1}$), V is the volume of the standard solution used (ml) and M is the mass of the adsorbent (g) used.

*Effect of Agitation Time*

A 50 ml of 30 mg $L^{-1}$ of the dye solution was measured into a 100 ml flask which contains 1g of the DPA and the flasks were maintained at 27 °C. The flasks were labelled for time difference of 5, 10, 15, 30, 45, 60 and 90 minutes and flasks were tightly covered and agitated for the appropriate time using incubator shaker. The un-adsorbed dye was determined with Beckman Coulter, DU-730 life science UV/Vis spectrophometer. The un-adsorbed dye was determined with Beckman Coulter, DU-730 life science UV/Vis spectrophometer. The quantity sorbed was calculated from eqn. 7.

*Effect of DPA Dosage on Adsorption*

A variable mass, 0.25, 0.5, 1, 2, 3 and 4 g of the DPA were weighed separately into 100 ml conical flasks. A 50 ml of the 30 mg $L^{-1}$ of each dye solution was added to each flask. The flasks were tightly covered, agitated on incubator shaker for 90 min and the solutions were filtered. The un-adsorbed dye was determined with Beckman Coulter, DU-730 life science UV/Vis spectrophometer. The quantity sorbed was calculated from eqn. 7.

*Thermodynamic Study*

A 2 g of the adsorbent was weighed into two sets of five conical flasks and 50 ml of 30 mg $L^{-1}$ of the dye solutions were measured into the flasks. The flasks were labelled for temperature difference of 35, 40, 50, 60 and 70°C. The flasks were tightly covered and heated at the appropriate temperatures using incubator shaker for the time interval of 5, 10, 15, 30, 45, 60 and 90 minutes at every temperature. The filtrates were treated for the quantity of dye adsorbed using eqn. 7.

*Adsorption Isotherms*

The adsorption data obtained were subjected to three different two-parameter isotherm equations in order to establish the relationship between the equilibrium concentration of the dyes in the liquid phase and in the solid phase (DPA); and to determine which of the isotherms best describe the adsorption process. These isothermal equations are:

a) Langmuir

$$\frac{C_e}{q_e} = \frac{1}{bq_m} + \left\{\frac{1}{q_m}\right\} C_e \qquad (08)$$

b) Freundlich

$$\log q_e = \log K_f + \frac{1}{n} \log C_e \qquad (09)$$

c) Temkin:-

$$q_e = B\ln A + B\ln C_e \qquad (10)$$

where $q_e$ is the quantity of sorbed at equilibrium (mg $g^{-1}$), Ce is the equilibrium concentration of adsorbate (mg $L^{-1}$). The Langmuir adsorption isotherm constants, b and $q_m$, were determined from the intercept and slope of the plot of $C_e/Q_e$ against $C_e$ [60]. The Freundlich adsorption isotherm was determined by plotting log $q_e$ against log $C_e$. The slope and intercept obtained from the graph were used to calculate the Freundlich constants, n and $K_f$ while $q_e$ was plotted against InCe in order to determine Temkin constants A (L $g^{-1}$) and B (mol $J^{-1}$) which are Temkin isotherm constant and constant related to heat of adsorption respectively. B = RT/b, where b is the Temkin constant related to heat of sorption (J $mol^{-1}$).

## Results and Discussion

The Table-1 summarised some of the characteristics of the AC produced from date palm seeds (DPA). The Table-1 showed that the AC produced has a good efficiency, ash content and volatile matter when compared to results of other researches. The % AC efficiency was 56.54 %, this value was relatively higher compared to the reported efficiency of 20.7% [24], 40% [25], 46.08 % [26] and 51% [27]. The Ash content is a reflection of the amount of inorganic substituent present and was obtained as 2.89 %. The ash content of most agricultural products is within 0.2-13.4 % [28]. Volatile matter is due to the presence of organic compounds present in the raw material. The volatile matter obtained was 22.21 %, which is higher than (20.9 %) [29]. Bulk density indicates the fibre content of the precursor, the lower the value the better for its regeneration upon use. The AC bulk density was 0.65 g $ml^{-1}$ which is within 0.45 g $ml^{-1}$ [30] and 0.864 g $ml^{-1}$ [31] reported by other researchers. The moisture content of the AC is 15.58 % which is slightly higher than some reported values 13.2% [28], 4.5% [16] and 9.8 % [15].

The AC has a moderately high surface area of 781.40 $m^2$ $g^{-1}$ which is higher than 342 $m^2$ $g^{-1}$ and 352 $m^2$ $g^{-1}$ for AC from some agricultural by-products but comparable to 760 $m^2$ $g^{-1}$ for commercial activated carbon (AC-a) [32]. This value is lower than 862.39 $m^2$ $g^{-1}$ [29] and 1141 $m^2$ $g^{-1}$ [24] reported for similar materials. Iodine number is the most fundamental parameter used to characterize activated carbon performance and it is a measure of activity level, the higher the number the higher the degree of activation. It is often reported in mg/g and typical values range between 500-1200 mg $g^{-1}$ [29]. The AC has moderate Iodine number (711.2 mg $g^{-1}$) and it is an indication of better performance as an adsorbent.

The result of CHN analysis (Table-1) showed that it contains 69.25 % C, 3.91 % H and 1.56 % N, most agricultural materials are within 41.23-84.50% C, 4.63-6.26% H and 0.7-4.10% N [15, 28]. The results of elemental analysis by XRF (Table-1) showed that P, Ca Na, S, Si, and K occurred as major constituents while Mg, Al, Mn and Ti as minor constituents. The FTIR spectra obtained (Fig. 2) were in agreement with the results reported for commercial granular activated carbons [33], activated carbon prepared from cherry stones [34] and activated carbon from coconut husk [20]. The FTIR spectra showed a prominent peak at 3465.93 $cm^{-1}$ that was attributed to the stretching frequency of O-H due to inter and intra molecular hydrogen bonding of polymeric compounds such as alcohols or phenols as in pectin, hemicelluloses, cellulose and lignin [35]. The peak observed at 2928.31 $cm^{-1}$ was associated with the stretching vibrations of C-H bond of methyl, methylene or methoxy group [36].The band in the region of ≈1600 $cm^{−1}$ has been observed by many previous researchers but has not been interpreted definitely, however, for most carbonaceous materials, C=C stretching absorption frequently occurs at this region [33, 37]. The spectrum in the region of 1164.00 $cm^{−1}$ and 1082.40 $cm^{−1}$ represented C-O stretching vibrations of functional groups such as alcohols, ethers, carboxylic acids and esters. The major absorption bands and assignments are summarised in Table-2.

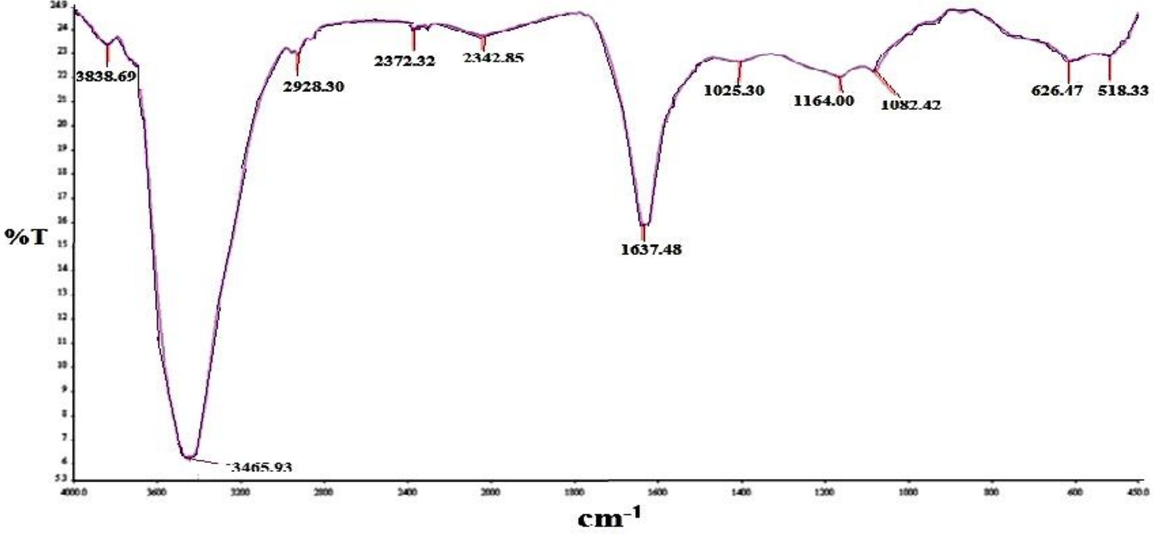

Fig. 2: FTIR spectra of DPA.

Table-1: Physico-chemical characterization of DPA and XRF analysis of AC.

| Properties | Value | Element | % |
|---|---|---|---|
| **Moisture content (%)** | **15.58** | **Na** | **2.324** |
| **Ash content (%)** | **2.89** | **S** | **1.588** |
| **Volatile matter (%)** | **22.21** | **Si** | **1.467** |
| **Surface area (m2/g)** | **781.40** | **Ca** | **6.649** |
| **Iodine number (mg/g)** | **711.2** | **Al** | **0.693** |
| **Bulk density (g/ml)** | **0.65** | **Fe** | **0.039** |
| **pH** | **6.6** | **K** | **1.210** |
| **Yield (%)** | **56.54** | **Ti** | **0.063** |
| **C (%)** | **69.25** | **Mn** | **0.071** |
| **H (%)** | **3.91** | **Mg** | **0.143** |
| **N (%)** | **1.56** | **P** | **10.397** |

Table-2: FTIR spectrum of DPA and their assignments.

| Peaks ($cm^{-1}$) | Assignment |
|---|---|
| **3834.69** | **O-H stretching vibration** |
| **2928.31** | **$CH_2$ stretching vibration** |
| **2372.32** | **C≡C stretching vibration** |
| **1637.48** | **C=C stretching vibration** |
| **1405.30** | **C-CH3 deformation** |
| **1164.00, 1082.40** | **C-O-H stretching vibrations** |
| **616.47, 518.33** | **C-O-H twist** |

### *Effect of Initial Dye concentration*

The influence of equilibrium concentration of the two dyes followed similar trend (Fig. 3). There was a general increase in adsorption of alizarin and fluorescein with increase in the equilibrium concentrations onto DPA up to a concentration of 30 mg $L^{-1}$ with 17.67 and 20.56 mg $g^{-1}$ respectively as the maximum quantity adsorbed when adsorption curves formed plateau after which the adsorption dropped. At lower initial concentrations, the process is concentration dependent and the ratio of the initial dye molecules to the available surface area is low but when the concentration is higher than 30 mg $L^{-1}$, the fractional adsorption become independent on the initial concentration. The gradual rise in the quantity adsorbed with increasing equilibrium concentrations are due partly to the availability of free adsorption sites on the DPA at lower dyes concentrations coupled with the effect of concentration gradient which is the main driving force for the adsorption process [38]. As the binding sites became exhausted, the uptake rate slowed down due to competition for decreasing available actives sites by dye ions [39].

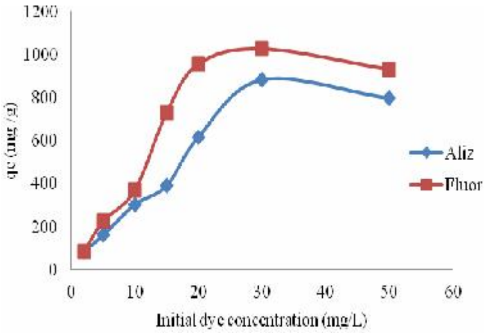

Fig. 3: Effect of initial dye concentration.

### *Effect of Agitation Time*

The plot of the effects of agitation time on the adsorption of the alizarin and fluorescein on DPA are depicted in Fig. 4. Two stages of adsorption were observed from Fig. 3; the first stage between 0 and 15 min representing fast uptake of dye molecules with 57.78% and 68.40% Alizarin and Fluorescein removal respectively and the second stage between 15 and 90 min with 61.04% and 71.00% Alizarin and Fluorescein removal respectively which represent a slow transfer of molecules onto the adsorption sites. The process of agitation of the adsorbate-adsorbent phase has the tendency of exposing active surfaces which otherwise, may be inaccessible. Similar observation was earlier reported [25, 31, 40, 41]. The optimum time for adsorption onto DPA is 90 min.

### *Effect of DPA Dose*

The effect of the quantity of DPA used on the adsorption of alizarin and fluorescein were studied, in which the amount of adsorbent was varied from 0.25 to 4 g while the dyes concentration were fixed at 30 mg $L^{-1}$. The net quantity of adsorbate removed increased with increasing mass of DPA which is attributed to an increase in the sorptive surface area and the availability of more active binding sites (Fig. 5). The net equilibrium amount adsorbed however is an expression of the efficiency of an adsorbent which may not show increase in the amount adsorbed per unit mass as the adsorbate dose increases [42]. However, the amount of dye adsorbed per unit mass of adsorbent decreased as the adsorbent dosage was increased from 0.25 to 4 g. This may be due partly to the inaccessibility of the active sites and partly to overlapping or aggregation of adsorption sites as the adsorbate dose increases [43, 44]. Thus with increasing adsorbent mass, the amount of dye adsorbed onto unit mass of adsorbent gets reduced, thus causing a decrease in $q_e$ value with increasing adsorbent mass concentration.

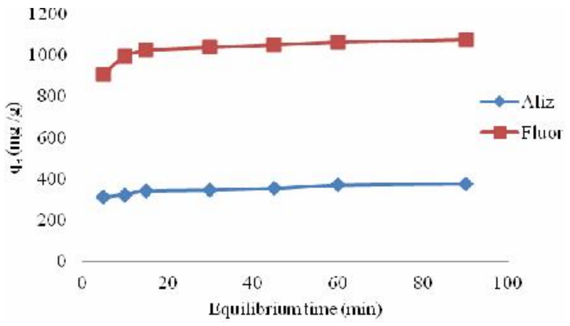

Fig. 4: Effect agitation time.

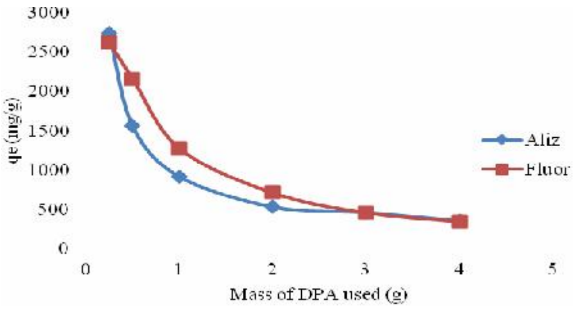

Fig. 5: Effect of adsorbate dose.

*Effect of Temperature*

The dependence of dye adsorption on temperature was studied within the temperature range of 35 to 70°C. The effect of temperature on the adsorption of fluorescein was insignificant but followed the same trend as the adsorption of alizarin which gave an S-like curve (Fig. 6). The S- like curve had two stages of fast and slow adsorption processes. The temperatures range from 35 to 40 and 50 to 60 °C represent sharp rise in the quantity adsorbed while curve between 40 to 50 °C represents slow rise in the quantity of dye molecules adsorbed. The higher removal due to increasing temperature may be attributed to chemical reaction taking place between the functional groups of the adsorbent and the dye [40]. More so, at higher temperatures there would be an increase in the mobility of the large molecules of dye ions thereby producing a swelling effect within the internal structure of the adsorbent. This enables the large dye molecules to penetrate the porous structure of DPA [7]. The increase in the quantity adsorbed with increasing temperature may suggest chemical interactions between the adsorbate and the adsorbent and accessibility of more active sites on DPA.

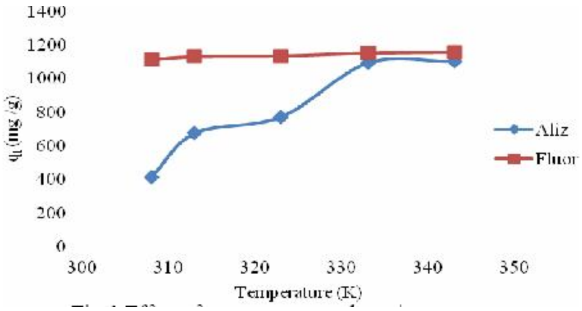

Fig. 6: Effect of Temperature on Adsorption.

*Adsorption Isotherms*

An adsorption isotherm represents the equilibrium relationship between the adsorbate concentration in the liquid phase and that on the adsorbent surface at a given condition. A number of isotherms have been developed to describe equilibrium relationships. In the present study, Langmuir, Freundlich and Temkin models were used to describe the equilibrium data. These data fitted well into all except Temkin model which yielded poor $R^2$ values for Alizarin and Fluorescein. Fig. 7a and 7b represent the plots of data into Langmuir and Freundlich equations. The tests of data indicated that the adsorption of alizarin and fluorescein on DPA are best described by Langmuir adsorption isotherm. The separation parameter, $K_L$, is an indication of level of interaction between the adsorbate and adsorbent [45]. The adsorption of a molecule onto an adsorbent may be described as unfavourable ($K_L$>1), linear ($K_L$=1), favourable (0< $K_L$<1) or irreversible ($K_L$<0) based on the calculated $K_L$ value.

$$K_L = \frac{1}{1+bC_0} \tag{01}$$

The $K_L$ for the dyes is less than unity indicating that the adsorption process was favourable. Therefore, DPA is an excellent adsorbent for the removal of alizarin and fluorescein. The isothermal constants and regression coefficients are summarised in Table-3.

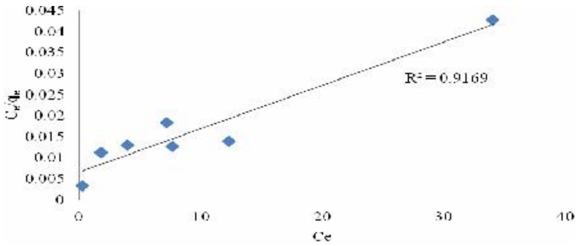

Fig. 7: (a) Linearized Langmuir for Alizarin.

*Adsorption Kinetic Study*

The data obtained from the influence of time on the adsorption of alizarin and fluorescein onto DPA were subjected to the pseudo-first order and pseudo-second order kinetics equations for a test of fitness of data and the plots of which gave Fig. 8 and 9 respectively. It was found that all the data fitted into pseudo-first and second order models. The linearity of the plots with $R^2$ values that are very close to unity indicates that the adsorption process followed pseudo-second order kinetic model better than the pseudo-first order model. A number of adsorption processes on activated charcoal have been reported to fit well into second order kinetic model

[7, 46, 47]. The Table-3 summarises the kinetics parameters for pseudo-first and second order models.

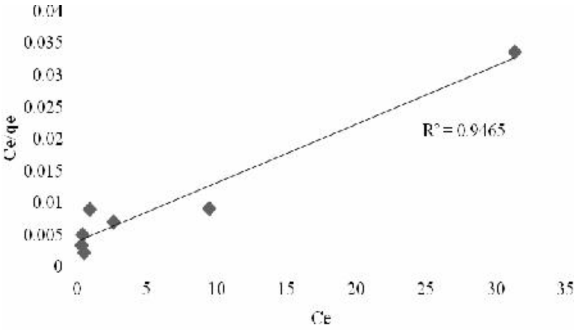

Fig. 7: (b) Linearized langmuir isotherm for Fluorescein.

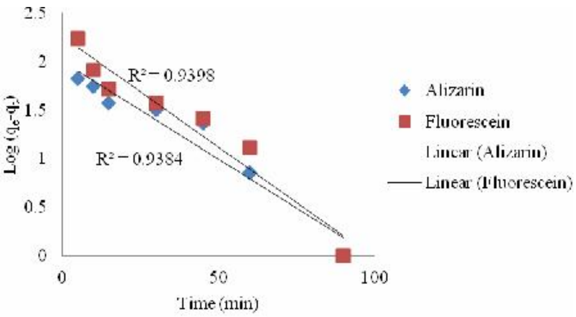

Fig. 8: Pseudo-first order of dyes onto DPA.

Table-3: Isothermal, kinetics constants and regression coefficients.

| Adsorption isotherm | | Alizarin | Fluorescein |
|---|---|---|---|
| | $R^2$ | 0.912 | 0.947 |
| Langmuir | $K_L$ (L/g) | 0.149 | 0.225 |
| | $q_m$ (mg/g) | 1000 | 1111.111 |
| | $R^2$ | 0.908 | 0.357 |
| Freundlich | $K_f$ (mg/g) | 197.651 | 396.28 |
| | n | 3.340 | 3.18 |
| | $R^2$ | 0.764 | 0.377 |
| Temkin | A (L/min) | 2.68 | 62.31 |
| | B | 167.40 | 133.20 |
| | $R^2$ | 0.938 | 0.939 |
| Pseudo-first order | $k_1$ ($min^{-1}$) | 0.047 | 0.052 |
| | $q_e$ (mg/g) | 100.29 | 178.24 |
| | $R^2$ | 0.999 | 0.962 |
| Pseudo-second order | $k_2$ (g/mg/min) | 0.0012 | 0.0027 |
| | $q_e$ (mg/g) | 384.62 | 1111.11 |

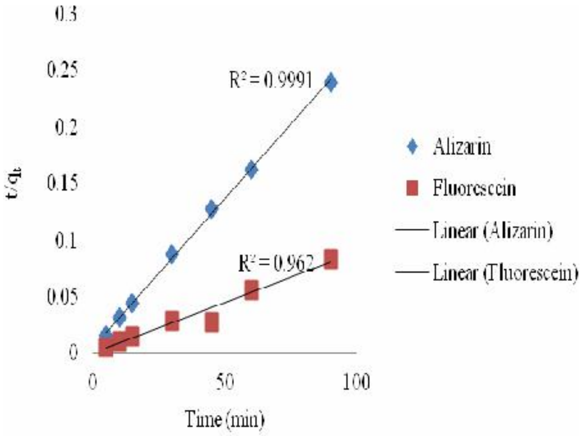

Fig. 9: Pseudo-second order plot of dyes on DPA.

*Thermodynamic Study*

In order to study the feasibility of the adsorption process, the thermodynamic parameters such as free energy, enthalpy and entropy changes were estimated from the following equations [48].

$$K = \frac{C_{Ae}}{C_e} \quad (02)$$

$$\Delta G = -RTInK \quad (03)$$

$$In\,K = \frac{\Delta S}{R} - \frac{\Delta H}{RT} \quad (04)$$

$$\Delta G = \Delta H - T\Delta S \quad (05)$$

where $C_e$ is the equilibrium concentration in solution in mg $L^{-1}$ and $C_{Ae}$ is the equilibrium concentration on the sorbent in mg $L^{-1}$ or equilibrium concentration of adsorbate A on the adsorbent and *K* is the equilibrium constant. The Gibbs free energy (ΔG) for the adsorption of alizarin and fluorescein onto DPA at all temperatures were obtained from Eq. 3 by substituting the K obtained from Eq. 2 and are presented in Table-4.

Table-4: Thermodynamic parameters for adsorption of alizarin and fluorescein on MGA.

| Temp. K | DPA | | | | | | | |
|---|---|---|---|---|---|---|---|---|
| | Alizarin | | | | Fluorescein | | | |
| | ΔG (Kj/mol) | ΔH (Kj/mol) | ΔS (Kj/mol) | $E_a$ (Kj/mol) | ΔG (Kj/mol) | ΔH (Kj/mol) | ΔS (Kj/mol) | $E_a$ (Kj/mol) |
| 308 | +2.464 | +49.36 | +0.15 | -8.19 | -2.727 | +3.67 | +0.021 | +21.43 |
| 313 | +0.511 | | | | -2.919 | | | |
| 323 | +0.172 | | | | -2.970 | | | |
| 333 | -2.750 | | | | -3.314 | | | |
| 343 | -2.910 | | | | -3.473 | | | |

The values of ΔH and ΔS were calculated from the slopes and intercepts of the plots of InK versus 1/T for alizarin and fluorescein (Fig. 10a and 10b respectively). These values are reported in Table-

4. From the pseudo-second order rate constant $k_2$, the activation energy $E_a$ for the adsorption of alizarin and fluorescein on DPA surface were determined using the Arrhenius equation.

$$\ln k_2 = \ln A - \frac{E_a}{RT} \qquad (06)$$

where, k is the rate constant, A is the Arrhenius constant, $E_a$ is the activation energy (Kj $mol^{-1}$), R is the gas constant (8.314 Jmol-1 $K^{-1}$) and T is the temperature (K). $E_a$ was obtained from a plot of $\ln k_2$ versus 1/T. The adsorption process is spontaneous for fluorescein for all temperatures studied but only at higher temperatures for alizarin due to negative ΔG values obtained. The efficiency of adsorption increases with increase in temperature as ΔG values decreases with increase in temperature. At higher temperatures, ions are easily desolvated and therefore their adsorption becomes more favourable [49, 50]. The endothermic in nature of the sorption processes is supported by the positive ΔH values and on the basis of magnitude of ΔH values the adsorptions of fluorescein and alizarin were by physical and physicochemical processes respectively (Table-4). The type of sorption can be explained in terms of the magnitude of ΔH. Generally, the ΔH values for physiosorption and chemisorption are within the range of 2.1 - 20.9 Kj $mol^{-1}$and 80 - 200 Kj $mol^{-1}$ respectively [51].

There could be structural exchange among the active sites of the adsorbents and the dyes which is responsible for an increased randomness during the adsorption of alizarin and fluorescein reflecting the affinity of DPA for dyes [15]. The positive ΔS value at higher ionic strength suggests spontaneous process. The increase in randomness at the adsorbent-adsorbate interface during the adsorption process leads to the increase in entropy and hence an overall positive ΔS. The adsorption process is therefore likely to occur spontaneously and more readily at high temperatures because $\Delta H > 0$ and $\Delta S > 0$ [52]. The $E_a$ obtained for fluorescein and alizarin on DPA are 21.43 Kj $mol^{-1}$ and -8.19 Kj $mol^{-1}$ respectively. The lower the $E_a$ value of a reaction process, the more probable it is spontaneous.

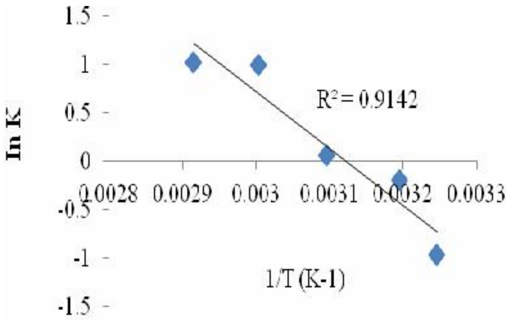

Fig. 10: (a) A graph of lnK against 1/T for Alizarin.

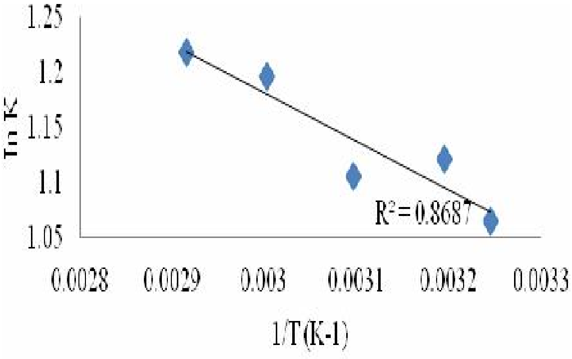

Fig. 10: (b) A graph of lnK versus 1/T for Fluorescein.

## Conclusion

The preparation of AC from DAP was achieved through one step process of carbonization and activation with 56.54% efficiency and moderately high surface area of 781.40 $m^2\ g^{-1}$. The performance was evaluated through batch equilibration of Alizarin and Fluorescein for the purpose of optimisation of adsorbent dose, dyes concentration and temperature conditions. The uptake increased with increasing agitation time, concentration and temperature. The adsorption equilibrium was attained in 90 minutes of agitation. The kinetic data obtained from this study showed good correlation coefficient for a pseudo-first and pseudo-second order kinetic model. The equilibrium data conformed well to the Langmuir isotherm with a high correlation coefficient close to unity, indicating that the adsorption of single dye solution onto surface of DPA followed a monolayer pattern. The activation energy $E_a$ of the adsorption process for alizarin and fluorescein on DPA were -8.19 and +21.43 Kj $mol^{-1}$ respectively, thermodynamic quantities such as Gibbs free energy (ΔG), the enthalpy (ΔH) and the entropy change of sorption (ΔS) were evaluated and indicated that the adsorption process was spontaneous and endothermic. Therefore, DPA can be considered as alternative biomass for the removal of single dye solution of alizarin and fluorescein since it was found to be effective; low cost; abundant and can be source locally.

Many catalytic processes, especially those used in organic synthesis, require transition metals which include manganese, iron, titanium etc. The prepared activated carbon contained varying concentrations of transition metals which may be useful in the catalytic processes. Therefore, in the present study the elemental analysis of this activated carbon is useful in the field of adsorption and catalysis

## Acknowledgements

The authors are grateful to Mr. S.A. Asala (the Chief Technologist), Mr J. Adamu and other technologist in the Department of Chemistry laboratory and Central Research laboratory, University of Ilorin for their support during the course of research work.

## References

1. V. Tharapong, S. Terachai and D. Somsak, Production of Activated Carbon from Palm-oil Shell by Pyrolysis and Steam Activation in a Fixed Bed Reactor, *Sci. Asia*, **25**, 211 (1999).
2. O. A. Olafadehan and D. S. Aribike, Treatment of Industrial Wastewater Effluent: Adsorption of Organic Compounds on Granular Activated Carbon, *J. Nig. Soc. Chem. Eng.*, **19** (1 & 2), 50, (2000).
3. V. K. Gupta, A. Mittal, L. Krishnan and V. Gajbe, Adsorption Kinetics and Column Operations for The Removal and Recovery of Malachite Green from Wastewater Using Bottom Ash, *Sep. Purif. Technol.*, **40**, 87 (2004).
4. P. Silvina, P. Viviana, R. Elsa and L. F. María, Elimination of Dyes from Aqueous Solutions using Iron Oxides and Chitosan as Adsorbents: A comparative study. *Quím. Nova*, **32**, 1239 (2009).
5. Z. Wu, H. Joo, I. S. Ahn, S. Haam, J. H. Kim and K. Lee, Organic Dye Adsorption on Mesoporous Hybrid gels. *Chem. Eng. J.*, **112**, 277 (2004).
6. L. Wang, A. Roitberg, C. Meuse and A. K. Gaigalas, Raman and FTIR Spectroscopies of Fluorescein in Solutions, *Spectrochim. Acta Part* A*: Molecular and Biomolecular Spectroscopy*, **57**, 1781 (2001).
7. A. K. Asiagwu, H. I. Owamah and V. O. Illoh, Kinetic and Thermodynamic Models for the Removal of Amino-phenol (dye) From Aqueous Solutions Using Groundnut (Arachis hypogea) Shells as the Biomass. *Adv. Applied Sci. Res.*, **3**, 2257 (2012).
8. H. Pignon-Metivier, C. Faur-Brasquet and P. Le Cloirec, Adsorption of Dyes onto Activated Carbon Cloth: Approach of Adsorption Mechanisms and Coupling of ACC with Ultra Filtration to Treat Coloured Wastewaters, *Sep. Purif. Tech.*, **31**, 3 (2003).
9. W. J. Weber, *Physico-Chemical Methods of Treatment of Water and Wastewater*, John Wiley and Sons Inc., p1175 (1978).
10. Y. Zhongren, E. James, R. Kishore, B. Gary, P. Marv, L. Ding, and M. Benito, Chemically Activated Carbon on a Fibre glass Substrate for removal of trace atrazine from water, *J. Mater. Chem.*, **16**, 3375 (2006).
11. WHO (World Health Organization) *International Agency for Research on Cancer. Monograph on Evaluation of Carcinogenic Risks to Human: Atrazine*. WHO, Geneva. Vol 73 (1999).
12. S. Arun, MSc, Department of Chemical Engineering, Mississippi State University, USA, 2002.
13. M. S. Jassim, and A. A. Khalid, Adsorption of 2, 4-dichlorophenoxyacetic acid onto Date Seeds Activated Carbon: equilibrium, Kinetic and Thermodynamic Studies, *Int. J. Chem. Sci.*, **10**, 677, (2012).
14. S. Koumaiti, K. Riahi, F. Ounaies and B. Ben Thayer, Kinetic Modelling of Liquid-Phase Adsorption of Sulfate onto Raw Date Palm Seeds, *J. Environ. Sci. Eng.*, **5**, 1570 (2011).
15. S. M. Mane, A. K. Vanjara and M. R. Sawant. Removal of Phenol from Wastewater Using Date Seed Carbon, *J. Chinese Chem. Soc.*, ***52***, 1117 (2005).
16. M. Salman, M. Athar, U. Shafique, M. I. Din, R. Rehman, A. Akram and S. Z. Ali, Adsorption Modelling of Alizarin Yellow on Untreated and Treated Charcoal, Turkish J. Eng. Env. Sci., **35**, 209 (2011).
17. C**.** Srinivasakannan and M. Z. Abu Baker, Production of activated carbon from rubber wood sawdust, *Biomass Bioenergy*, **27**, 89 (2004).
18. Y. A. Alhamed and H. S. Bamufleh, Sulfur removal from model diesel fuel using granular activated carbon from dates' stones activated by $ZnCl_2$ *Fuel.* **88**, 87 (2009).
19. B. H. Hameed, A. T. M. Din and A. L. Ahmad, Adsorption of methylene blue onto bamboo-based activated carbon: Kinetics and equilibrium studies, *J. Hazard. Mater.*, **141**, 819 (2007).
20. I. A. W. Tan, A. L. Ahmad and B. H. Hameed, Preparation of activated carbon from coconut

husk: Optimization study on removal of 2,4,6-Trichlorophenol using response surface methodology, *J. Hazard. Mater.*, **153**, 709 (2008).

21. R. Torregrosa Macia, J. M. Martin Martinez, and M. C. Mittelmeijer-Hazeleger, Porous texture of activated carbons modified with carbohydrates *Carbon***, 35**, 447 (1997).
22. K. Yang, J. Peng, C. Srinivasakannan, L. Zhang, H. Xia and X. Duan, Preparation of high surface area activated carbon from coconut shells using microwave heating, *Bioresour. Technol.,* **101**, 6163 (2010).
23. F. Rodriguez-Reinoso, M. Molina-Sabio and M. T. Gonzalez, The use of steam and CO2 as activating agents in the preparation of activated carbons *Carbon***, 33**, 15 (1995).
24. B. H. Hameed, I. A. W. Tan, and A. L. Ahmad, Preparation of oil palm empty fruit bunch-based activated carbon for removal of 2,4,6-Trichlorophenol: optimization using response surface methodology, *J. Hazard. Mater.***, 164**, 1316, (2009).
25. M. A. Ahmad and R. Alrozi, Optimization of preparation conditions for mangosteen peel-based activated carbons for the removal of remazol brilliant blue R using response surface methodology. Chemical Eng. J.**, 165**, 883 (2010).
26. S. D. Faust and O. M. Aly, *Chemistry of Water Treatment*, Butterwoths Publishers, Boston, London, Wellington, p211 (1983).
27. J. N. Sahu, J. Achrya and B. C. Meikap, Optimization of production conditions for activated carbons from Tamarind wood by zinc chloride using response surface methodology. *Bioresour. Technol.*, **101**, 1974 (2010).
28. O. Ioannidou and A. Zabaniotou, Agricultural residues as precursors for activated carbon production-A review. *Renew. Sustainable Energy Rev.*, **11(9)**, 1966 (2007).
29. B. J. Raffiea, P. N. Palanisamy and P. Sivakumar, Preparation and characterization of activated carbon from *Thevetia peruviana* for the removal of dyes from textile waste water. *Adv. Applied Sci. Res.*, **3**, 377 (2012).
30. B. Y. Nale, J. A. Kagbu, A. Uzairu, E. T. Nwankwere, S. Saidu and H. Musa, Kinetic and Equilibrium Studies of the Adsorption of Lead(II) and Nickel(II) ions from aqueous solutions on Activated Carbon Prepared from Maize Cob, *Adv. Appl. Sci. Res.*, **3,** 302 (2012).
31. Y. B. Onundi, A. A. Mamun, M. F. Al. Khatib, M. A. Al-Saadi, and A. M. Suleyman, Heavy metals removal from synthetic wastewater by a novel nano-size composite adsorbent. *Int. J. Environ.Sci. Tech.*, **8**, 799 (2011).
32. Z. Ionannou and J. Simitzis, Adsorption of methylene blue onto activated carbons based on agricultural by-products: equilibrium and kinetic studies. *Water Sci. Technol.*, **67**, 1688 (2013).
33. M. Jung, K, Ahn, Y. Lee, K. Kim, J. Rhee, J. T. Park and K. Paeng, Adsorption characteristics of phenol and chlorophenols on granular activated carbon (GAC), *Microchem. J.*, **70**, 123 (2001).
34. M. Olivares-Mar´ın, C. Fern´andez-Gonz´alez, A. Mac´ıas-Garc´ıa and V. G´omez-Serrano, Preparation of activated carbons from cherry stones by activation with potassium hydroxide., *Appl. Surf. Sci.*, **252**, 5980 (2006).
35. M. Iqbal, A. Saeed and S. I. Zafar, FTIR spectrophotometry, kinetics and adsorption isotherm modeling, ion exchange, and EDX analysis for understanding the mechanism of $Cd^{2+}$ and $Pb^{2+}$ removal by mango peel waste. *J. Hazard. Mater.*, **164**, 161 (2008).
36. N. Feng, X. Guo and S. Liang, Adsorption study of copper (II) by chemically modified orange peel. *J. Hazard. Mater.*, **164**, 1286 (2008).
37. A. Florido, C. Valderrama, J. A. Arévalo I. Casas, M. Martínez and N. Miralles, Application of two sites non-equilibrium sorption model for the removal of Cu (II) onto grape stalk wastes in a fixed-bed column. *Chem. Engr. J.*, 156, 298 (2009).
38. S. Mishra, D. J. Prakash and G. Ramakrishna, Characterization and Utilization of Mahua Oil Cake–A new Adsorbent for the Removal of Congo red Dye from Aqueous Phase. *Elect. J. Env. Agric. Food Chem.*, **8**, 425 (2009).
39. S. Gupta, D. Kumar and J. P. Gaur, Kinetic and isotherm modeling of lead (II) sorption onto some waste plant materials, *Chemical Eng J.*, **148**, 226 (2008).
40. T. P. S. W. Sumanjit and K. Ishu, Removal of Rhodamine-B by adsorption on walnut shell charcoal, *J. Surface Sci. Technol.*, **24,** 179 (2007).
41. M. A. O. Badmus, T. O. K. Audu and B. U. Anyata, Removal of lead ion from industrial wastewaters by activated carbon prepared from periwinkle Shells (Typanotonusfuscatus). *Turkish J. Eng. Env. Sci.*, **31**, 251 (2007).
42. N. Nasuha, B. H. Hameed and A. T. M. Din, Rejected tea as a potential low-cost adsorbent for the removal of methylene blue. *J. Hazard. Mater.*, **175**, 126 (2010).
43. G. Crini, H. Peindy, F. Gilbert and C. Robert, Removal of C.I. Basic Green (Malachite) from aqueous solutions by adsorption using cyclo

dextrin-based adsorbent, kinetic and equilibrium studies. *Sep. purif. Technol.,* **53**, 97 (2007).

44. S. T. Akar and A. S. Özcan, Biosorption of a reactive textile dye from aqueous solutions utilizing an agro-waste, *Desalination*, **249**, 757 (2009).
45. K. G. Bhattacharyya and S. Sen Gupta, Pb(II) uptake by Kaolinite and Montmorillonite in Aqueous Medium: Influence of Acid Activation of the Clays, *Colloids Surf A Physicochem Eng Asp*, **277**(1&3), 191 (2006).
46. N. K. Amin, Removal of reactive dye from aqueous solutions by adsorption onto activated carbons prepared from sugarcane bagasse pith, *Desalination,* **223**, 152 (2008).
47. A. L. Prasad and S. Thirumalisamy, Adsorption of hazardous cationic dyes from aqueous solution onto *Acacia nilotica* leaves as an eco-friendly adsorbent, *Sustain. Environ. Res.*, **22**, 113 (2012).
48. M. G. Sujana, H. K. Pradhan and S. Anand, Studies on sorption of some geomaterials for fluoride removal from aqueous solutions. *J. Hazard. Mater.,* **161**, 120 (2009).
49. C. Chen and X. Wang, Adsorption of Ni (II) from aqueous solution using oxidized multiwall carbon nanotubes. *Ind. Eng. Chem. Res.,* **45**, 9144 (2006).
50. R. Qadeer, Adsorption of Ruthenium ions on activated charcoal: influence of temperature on the kinetics of the adsorption Process. *J. Zhejiang Univ. Sci. B.,* **6**, 353 (2005).
51. Y. Liu and Y. J. Liu, Biosorption isotherms, kinetics and thermodynamics, *Sep. Purif. Technol.,* **61**, 229 (2008).
52. F. K. Bangash and A. Manaf, Dyes Removal from Aqeous Solution Using Wood Activated Charcoal of Bombax Cieba Tree, *J. Chinese Soc.,* **52**, 489 (2005).
53. O. P. Fapetu, Production of Carbon from Biomass for Industrial and Metallurgical Process. *Nig. J. Eng. Manag.*, **1**, 34 (2000).
54. P. R. Hesse, *A Textbook of Soil Chemical Analysis, Illustrated*. Chem. Pub. Co., John Murray, London, (1997)
55. ASTM D2866. *Test method for total ash content of activated carbon*. In: 2006 Annual Book of ASTM Standard. Vol. 15.01. American Society for Testing and Materials, West Conshohocken, PA.
56. S. Yoshiguki and K. Yukata, Pyrolysis of plant, animal and human waste: physical and chemical characterization of the pyrolytic product. *Bioresour. Technol.*, **90**, 241 (2003).
57. www.scribd.com/doc/44493885/Test-method for Activated- Carbon-86 retrieved on 16/11/2012.
58. ASTM D4607. *Test method for the determination of iodine number of activated carbon*. In: 2006 Annual Book of ASTM Standard. Vol. 15.01. American Society for Testing and Materials, West Conshohocken, PA.
59. F. A. Adekola, N. Abdus-Salam and L. B. Abdul-Rauf, Removal of Arsenic from Aqueous solution by Synthetic Hematite, *J. Chem. Soc. Nig.,* **36**, 52 (2011).
60. N. Abdus-Salam and A. D. Itiola, Potential Application of Termite Mound for Adsorption and Removal of Pb(II) from Aqueous Solutions. *J. Iran. Chem. Soc.,* **9**, 373 (2012).